ACS OMEGA

http://pubs.acs.org/journal/acsodf

Article

Exploring the Evolution Mechanism of Sulfur Vacancies by Investigating the Role of Vacancy Defects in the Interaction between H_2S and the FeS(001) Surface

Jingxuan Liang, Xiangli Wen, Shikai Wei, and Shuqi Zheng*

Cite This: *ACS Omega* 2021, 6, 19212−19221

Read Online

ACCESS | Metrics & More | Article Recommendations | Supporting Information

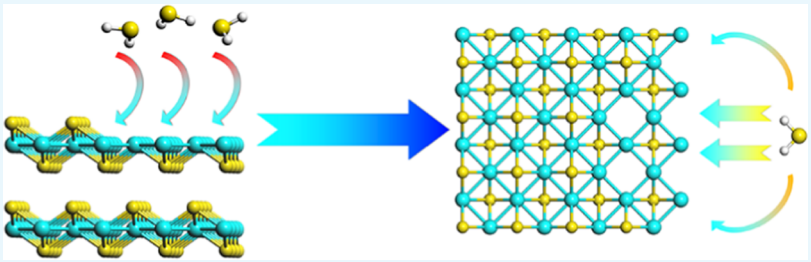

ABSTRACT: Vacancy defects are inherent point defects in materials. In this study, we investigate the role of Fe vacancy (V_{Fe}) and S vacancy (V_S) in the interaction (adsorption, dissociation, and diffusion) between H_2S and the FeS(001) surface using the dispersion-corrected density functional theory (DFT-D2) method. V_{Fe} promotes the dissociation of H_2S but slightly hinders the dissociation of HS. Compared with the perfect surface (2.08 and 1.15 eV), the dissociation energy barrier of H_2S is reduced to 1.56 eV, and HS is increased to 1.25 eV. Meanwhile, S vacancy (V_S) significantly facilitates the adsorption and dissociation of H_2S, which not only reduces the dissociation energy barriers of H_2S and HS to 0.07 and 0.11 eV, respectively, but also changes the dissociation process of H_2S from an endothermic process to a spontaneous exothermic one. Furthermore, V_{Fe} can promote the hydrogen (H) diffusion process from the surface into the matrix and reduce the energy barrier of the rate-limiting step from 1.12 to 0.26 eV. But it is very hard for H atoms gathered around V_S to diffuse into the matrix, especially the energy barrier of the rate-limiting step increases to 1.89 eV. Finally, we propose that V_S on the FeS(001) surface is intensely difficult to form and exist in the actual environment through the calculation results.

1. INTRODUCTION

H_2S corrosion is the most dangerous factor in the corrosion of equipment in oil and gas fields with high sulfur content. As a highly toxic gas, H_2S not only seriously threatens the routine use of equipment and pipeline steel but also directly threatens the safety of human life.[1,2] When steel is used in the H_2S environment, pitting corrosion, local corrosion, uniform corrosion, linear corrosion, stress corrosion cracking, and hydrogen-induced cracking occur easily.[3] In the 1980s, Canadian scholars found that corrosion products in H_2S environments were more complex than other corrosion environments. Especially, when iron-base alloys contacted the wet H_2S environment, corrosion product films would immediately form on the surface. The types of corrosion products were intricate and varied, and they often existed in the form of mixed crystals, mainly iron sulfide compounds with nonstoichiometry.[4,5]

Mackinawite (FeS) is an exceptionally crucial iron sulfide compound. It is the initial metastable corrosion product formed by steel in a humid H_2S environment at low temperatures, while it is also the main corrosion product.[6] Due to the strong reducibility, FeS is readily oxidized and converted into other more stable iron sulfide compounds.[7] Consequently, FeS is regarded as the forerunner of other iron sulfide compounds formed in deposition and hydrothermal systems, including pyrite (FeS_2), pyrrhotite (Fe_7S_8), and greigite (Fe_3S_4).[8] Besides, recent studies have shown that FeS exhibits typical metallic characteristics.[9] In a wet H_2S environment, the reaction at the iron sulfide compounds/H_2S interface has a vast influence on the formation of subsequent corrosion products and the transition between corrosion products.[10−13] A prior study discovered that in the Fe−H_2S−H_2O environment at a high temperature, the crystal evolution sequence of iron sulfide compounds is as follows: mackinawite → pyrrhotite → pyrite; troilite → pyrrhotite → pyrite.[14] In addition, FeS gradually transforms into pyrrhotite

Received: May 20, 2021
Accepted: July 1, 2021
Published: July 13, 2021

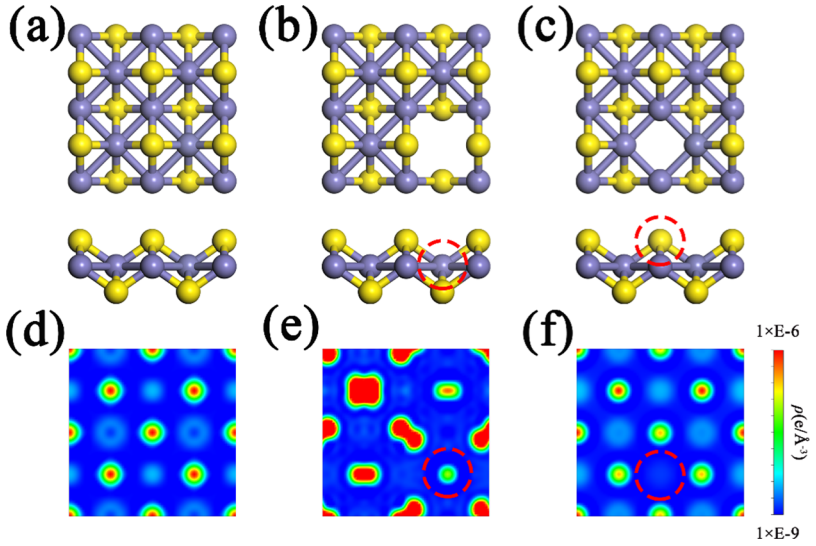

Figure 1. Top and front views (a–c) of the surface structures of perfect and vacancy-defective FeS(001) surfaces. Red dotted lines represent V_{Fe} and V_S, respectively. The charge density of perfect (d), vacancy-defective-Fe (e), and vacancy-defective-S (f) FeS(001) surfaces.

as the temperatures increase.[15] The H atoms generated by H_2S dissociation further diffuse from the surface to the interior of the matrix and gather at H traps such as defects and inclusions to form H_2, thus generating hydrogen bubbling or cracking.[16] Bai et al. studied the hydrogen escape behavior of FeS under different hydrogen charging conditions through the pyrolysis adsorption test, and the results showed that H diffused from grain boundary/dislocation to vacancies in the metal and that FeS had no obstruction to hydrogen permeation.[17]

The formation and transformation of FeS and its hydrogen resistance properties in the H_2S environment have been studied in detail experimentally. However, it is difficult to determine the interaction between H_2S and the low-dimensional surface of FeS from a microscopic point of view through the existing experimental techniques. Density functional theory (DFT) can provide an understanding of the interactions between small molecules and surfaces at the molecular level. In recent years, DFT has been widely used to study the adsorption/dissociation process of molecules and charge transfer between molecules and substrates. An FeS crystal has a tetragonal structure. Fe atoms are connected to four equidistant S atoms in a tetragonal lattice by tetrahedral coordination to form an equilateral tetrahedral layered structure stacked along the *z*-axis and stabilized by vdW force.[18] FeS is usually layered, so FeS is characterized by surface activity and high specific surface area like other two-dimensional layered materials.[19] In the past, some scholars have studied the interaction between some small molecules and diverse low-dimensional surfaces of FeS by the DFT method. Dzade et al. systematically studied the adsorption/dissociation of various small molecules on diverse low-dimensional surfaces of FeS.[20−24] The adsorption energy of small molecules at different adsorption sites on diverse low-dimensional surfaces was investigated, and the dissociation of small molecules was analyzed. The calculation results reported that NO_x, CO_2, H_2O, $C_3H_7NO_2S$, and C_4H_4S are more likely to dissociate on the most unstable FeS(111) surface. Meanwhile, the dissociation energy barrier of these molecules is the largest on the FeS(001) surface. Whereafter, further studies found that preadsorption of O_2/O atoms on diverse low-dimensional surfaces would promote the subsequent adsorption and dissociation of H_2O.[25] Moreover, Krishnamoorthy of MIT suggested the effect of the insertion of H_2 and H atoms in the gap between the FeS layers and the insertion of H atoms in the Fe vacancy on the tensile strength and elastic modulus of the matrix.[26] Recently, Wen et al. calculated the adsorption and dissociation processes of H_2S on diverse low-dimensional surfaces of FeS in corrosive environments.[27] The results demonstrated that H_2S had the lowest dissociation energy barrier on the FeS(011) surface and the highest on the FeS(001) surface.

It is widely known that crystal defects exist in any material.[28] Vacancy is an inherent point defect in a crystal structure. The existence of vacancy defects has a considerable effect on the reactivity of a surface.[29] For instance, the presence of S vacancies on the pyrite(100) surface not only promoted the adsorption of formamide but also facilitated the transition of amino acid from a zwitterionic species to an anionic species.[30,31] Sahraei et al. found that the vacancy defects on the ZnS(110) surface can change the hydrophilicity of the surface and also prompt the conversion of amino acid from neutral to zwitterionic.[32,33] Ward et al. revealed that pure FeS could be described by $FeS_{0.94}$.[34] Furthermore, crystallographic evidence found by Taylor and Finger et al. confirmed that FeS was sulfur-deficient (FeS_{1-x}, typically $0 \leq x \leq 0.07$).[35] This may be caused by the existence of V_S or the incorporation of interstitial metal atoms. In most calculations, a perfect FeS surface has been emphasized with attention. However, the influence of vacancy defects on the adsorption, dissociation, and H diffusion behavior of H_2S on the FeS surface is rarely reported. In view of the metastable nature of FeS, surface defects are very possible to form in the actual environment. Exploring the adsorption/dissociation and diffusion processes of H_2S on the vacancy-defective FeS surface by the DFT method can be used to guide the experiment. Besides, this allows us to further enhance the understanding of the hydrogen barrier properties of FeS and the influence of vacancy defects on the subsequent formation and transformation of iron sulfide compounds from the microscopic perspective.

In this work, we investigated the impact of V_{Fe} and V_S on the adsorption and dissociation processes of H_2S on the most

https://doi.org/10.1021/acsomega.1c02639
ACS Omega 2021, 6, 19212−19221

stable (001) surface of FeS. Besides, the diffusion energy barrier of the H atom from the surface into the matrix was calculated. In the end, according to the calculation results, we found that V_S on the FeS(001) surface is extremely difficult to form and exist in the actual environment.

2. RESULTS AND DISCUSSION

2.1. Properties of FeS(001) Surfaces. First, according to the vacancy formation energy formula, we calculate the formation energies of V_{Fe} and V_S of the FeS(001) surface. The results indicate that the formation energies of V_{Fe} and V_S are 1.34 and 3.91 eV, respectively. The top and front views of perfect and vacancy-defective FeS(001) surfaces are shown in Figure 1a−c. The red dotted lines represent V_{Fe} and V_S. Among them, V_{Fe} is in the second atomic layer and V_S is in the first atomic layer. Since vacancy defects are vacant in different layered positions, the charge density distribution is carried out to assess the change of the surface electronic structure. The charge density distribution of perfect and vacancy-defective FeS(001) surfaces is shown in Figure 1d−f. Blue and red represent the areas with lower and higher charge densities, respectively. The red dotted lines in the figure represent the location of vacancy defects. It can be clearly seen that a region with considerably low charge density is formed around the vacancy defects. Besides, the charge density around V_S decreases more obviously, which has a greater influence on the charge density distribution of the FeS(001) surface.

Moreover, we also calculated that the formation energy of the V_S of the third atomic layer is equal to that of the first atomic layer, but the result shows that V_S in the third atomic layer has almost no effect on the surface charge density distribution and the adsorption of H_2S. Therefore, our study focused on the V_S located in the first atomic layer and the V_{Fe} located in the second atomic layer, which are relatively close to the surface.

2.2. Adsorption of H_2S. Figure S1b−d shows the possible adsorption sites of different FeS(001) surfaces and dissolution sites in the matrix. Table S1 lists the related parameters of different adsorbents after they are stably adsorbed on different surfaces. Table 1 lists the structural parameters of the most stable adsorption configurations, where d (Å) expresses the distance between adsorbents and the surface. Figure 2 shows the top view, front view, DCD, and adsorption energy of H_2S stably adsorbed on perfect and vacancy-defective FeS(001) surfaces. The yellow and blue areas in the DCD represent the areas of charge increase and loss, respectively.

The stable adsorption site of H_2S on perfect and vacancy-defective-Fe FeS(001) surfaces are all Fe-B sites. However, on the vacancy-defective-Fe FeS(001) surface, the adsorption energy of H_2S decreases slightly, which reveals that the existence of V_{Fe} slightly decreases the adsorption capacity of H_2S. Nevertheless, the presence of V_{Fe} does not change the stable adsorption location and configuration of H_2S. The bond length, bond angle, and the distance between H_2S and the surface are almost identical to those of the perfect surface after H_2S was stably adsorbed on the vacancy-defective-Fe FeS(001) surface. Since the adsorption of H_2S on the FeS(001) surface itself is weak physical adsorption, and V_{Fe} is in the second atomic layer, so it is arduous to affect the adsorption process of H_2S on the surface. Besides, it can also be seen from the DCD that the charge transfer between H_2S and the vacancy-defective-Fe FeS(001) surface is basically the same as that between H_2S and the perfect FeS(001) surface.

Table 1. Structural Parameters of Different Adsorbates Stably Adsorbed on Different FeS(001) Surfaces

adsorbate	adsorption spot	d (Å)	[a]HSH (deg)	d (H−S) (Å)	E_{ads} (eV)
		Perfect FeS(001)			
H_2S	Fe-B[a]	2.794	91.346	1.352; 1.352	−0.23
HS	S-T[b]	2.157	–	1.357	−1.27
H + HS	Fe-B + S-T	1.665; 2.191	–	1.357	1.63
H + S	Fe-B + S-T	1.681; 1.942	–	–	−0.36
		Vacancy-Defective-Fe FeS(001)			
H_2S	Fe-B	2.781	91.570	1.352; 1.352	−0.19
HS	S-T	2.188	–	1.359	−1.43
H + HS	Fe-B + S-T	1.509; 2.187	–	1.355	1.33
H + S	Fe-V[c] + S-T	1.936; –	–	–	−0.48
		Vacancy-Defective-S FeS(001)			
H_2S	S-V	–	87.169	1.402; 1.403	−1.21
HS	S-V	–	–	1.376	−4.83
H + HS	Fe-B + S-V	1.601; –	–	1.377	−1.84
H + S	Fe-B + S-V	1.668; –	–	–	−4.96

[a]B: represents the bridge site. [b]T: represents the top site. [c]V: represents the location of the vacancy defect.

On the vacancy-defective-S FeS(001) surface, H_2S is stably and vertically adsorbed at the S-V site and has evident hybridization with the surface. The adsorption energy of H_2S increases to −1.21 eV. As one can see from the DCD, the H atom in H_2S takes some electrons from the S atom in H_2S, which is different from the charge transfer of H_2S after it is stably adsorbed on other surfaces. In addition, part of the charge from the S atom in H_2S is also transferred to the Fe atom of FeS. The transfer of charge further proves that there is a strong interaction between H_2S and the vacancy-defective-S FeS(001) surface, which may be caused by the reduction of the charge density prompted by V_S as mentioned above.

On the other hand, it can be seen from the structural parameters, compared with the perfect and vacancy-defective-Fe FeS(001) surfaces, the bond length of H_2S increases and the bond angle decreases on the vacancy-defective-S FeS(001) surface, proposing that these states may be the precursors of H_2S dissociation. This also provides some evidence from the side that the existence of V_S may promote the dissociation process of H_2S.

2.3. Dissociation of H_2S. In this work, CI-NEB is applied to calculate the maximum dissociation barrier E_a and the minimum energy paths (MEPs) of H_2S and HS. The adsorption energies and related parameters of HS + H and S + H after stable co-adsorption on different surfaces were calculated, as shown in Table 1. The top views of the IS_i, FS_i, and TS_i configurations of MEPs where H_2S and HS dissociate on the vacancy-defective FeS(001) surface are shown in Figures 3 and 4. Meanwhile, Table 2 lists the E_a and ΔE of the H_2S dissociation reaction. The energy barriers E_{a1} and E_{a2} as well as the transition state configurations on the perfect FeS(001) surface in this work are consistent with the previous calculations of our group (2.06 and 1.23 eV),[27] which also proves the validity of our work.

The MEPs of H_2S dissociated on the vacancy-defective-Fe FeS(001) surface are shown in Figure 3. The dissociation

https://doi.org/10.1021/acsomega.1c02639
ACS Omega 2021, 6, 19212−19221

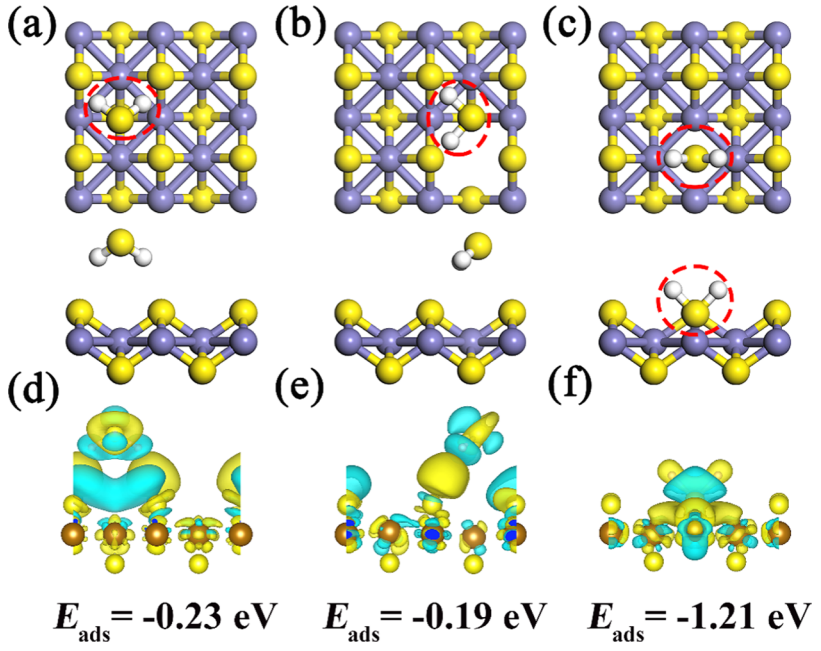

Figure 2. Different views of the stable adsorption texture of H_2S on perfect (a), vacancy-defective-Fe (b), and vacancy-defective-S (c) FeS(001) surfaces. (d–f) The corresponding DCD.

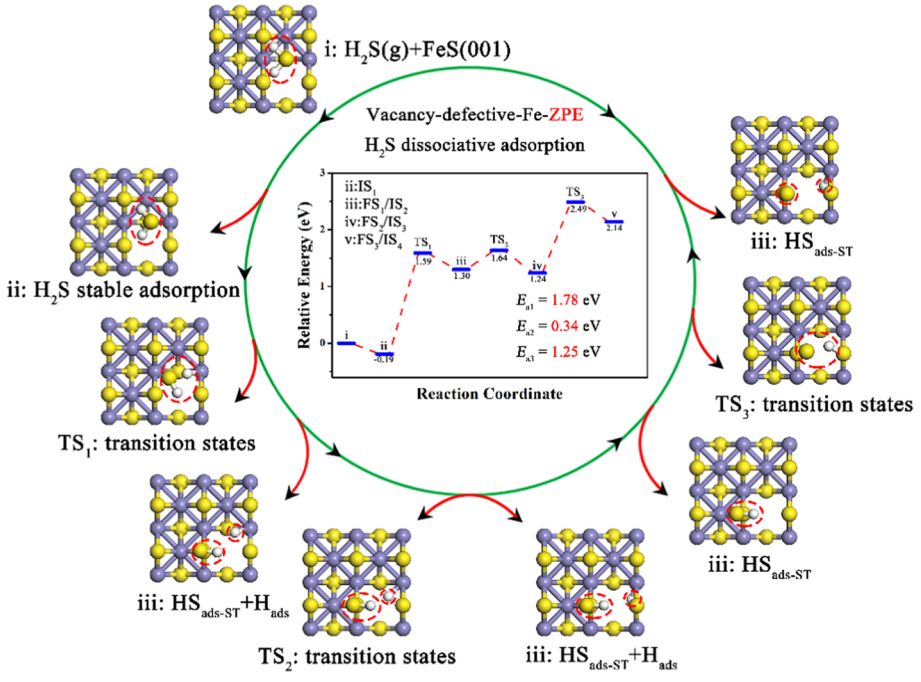

Figure 3. Most beneficial path for the dissociation of H_2S on the vacancy-defective-Fe FeS(001) surface.

process of H_2S goes through four steps: (a) H_2S is stably adsorbed at the Fe-B site near V_{Fe} by releasing an energy of 0.19 eV. (b) H_2S rotates horizontally, breaking an H–S bond away from V_{Fe}. Then, the H atom breaks off from H_2S, diffusing to the nearest Fe atom and forms a bond with it, while HS diffuses directly to the nearest S-T position. The energy barrier to be overcome for this process is 1.57 eV. (c) The isolated H atom diffuses from V_{Fe} to the interior of the matrix by overcoming an energy barrier of 0.34 eV. Meanwhile, HS does not change and still adsorbs at the original S-T site. (d) HS further overcomes an energy barrier of 1.25 eV and decomposes into S + H. After TS_3, the H atom continues to diffuse into the matrix through V_{Fe} and the S atom is still adsorbed at the S-T site. The stable dissolution site is the same as that of the H atom separated by H_2S in the first order. It can be seen from Table 2 that compared with the perfect surface, the dissociation energy barriers E_{a1} of H_2S decrease and E_{a2} increase to some extent, but the change is not conspicuous. The results imply that V_{Fe} has little influence on the dissociation reaction of H_2S. It is worth mentioning that although the energy barrier of H_2S dissociation does not change observably, we found that all H atoms dissociated from H_2S can diffuse into the matrix through V_{Fe}, which provides

https://doi.org/10.1021/acsomega.1c02639
ACS Omega 2021, 6, 19212–19221

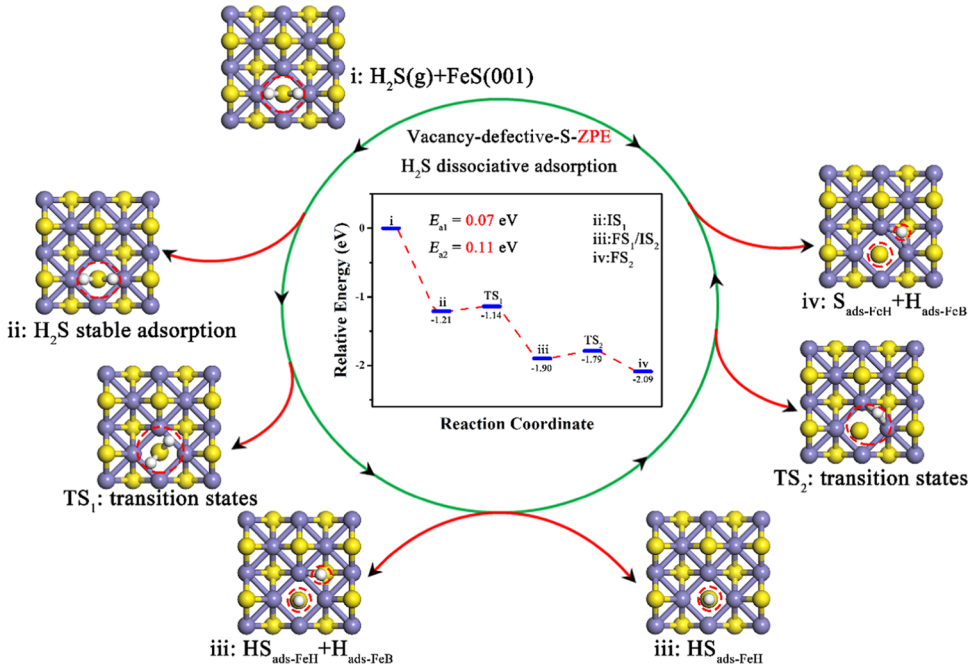

Figure 4. Most beneficial path for the dissociation of H_2S on the vacancy-defective-S FeS(001) surface.

Table 2. Reaction Heat (ΔE) and Dissociation Energy (E_a) of the Dissociation Steps of H_2S on the Perfect and Vacancy-Defective FeS(001) Surfaces

	perform ZPE		no ZPE	
reaction coordinate	$E_{a\text{-ZPE}}$ (eV)	$\Delta E_{\text{-ZPE}}$ (eV)	E_a (eV)	ΔE (eV)
Perfect FeS(001)				
P_1: $IS_1 \rightarrow TS_1 \rightarrow FS_1$	2.08	1.77	2.19	1.86
P_2: $IS_2 \rightarrow TS_2 \rightarrow FS_2$	1.15	0.83	1.19	0.91
Vacancy-Defective-Fe FeS(001)				
P_1: $IS_1 \rightarrow TS_1 \rightarrow FS_1$	1.56	1.49	1.90	1.56
P_2: $IS_2 \rightarrow TS_2 \rightarrow FS_2$	0.34	−0.06	0.29	−0.05
P_3: $IS_3 \rightarrow TS_3 \rightarrow FS_3$	1.25	0.90	1.32	0.95
Vacancy-Defective-S FeS(001)				
P_1: $IS_1 \rightarrow TS_1 \rightarrow FS_1$	0.07	−0.69	0.13	−0.63
P_2: $IS_2 \rightarrow TS_2 \rightarrow FS_2$	0.11	−0.19	0.18	−0.13

some guidance for our subsequent study on the H diffusion process from the surface into the matrix.

The MEPs of H_2S completely dissociated on the vacancy-defective-S FeS(001) surface are shown in Figure 4. In this process, the dissociation of H_2S can be divided into three steps: (a) H_2S is stably adsorbed at the S-V site and the adsorption energy is −1.21 eV. (b) H_2S directly rotates 45° in the horizontal direction at S-V, and then a H−S bond breaks. The liberated H atom diffuses to the nearest Fe-B site and gets adsorbed stably, while HS continues to be adsorbed stably at the original S-V site. The energy barrier to be overcome for this process is 0.07 eV. (c) HS further overcomes an energy barrier of 0.11 eV and decomposes into S + H. Similar to the first H atom, the H atom split from HS also diffuses to the nearest Fe-B site for stable adsorption, while the S atom continues to be adsorbed stably at the S-V site.

Compared with the perfect surface, the dissociation energy barriers E_{a1} and E_{a2} of H_2S on the vacancy-defective-S FeS(001) surface are intensely reduced, and the whole dissociation process changes from endothermic to exothermic. The existence of V_S greatly promotes the dissociation process of H_2S. Also, H_2S can be dissociated directly through two dehydrogenation processes at the original adsorption site, making the dissociation process more concise. The calculations demonstrate that V_S has a strong adsorption capacity for H_2S, which is also caused by the extreme decrease of charge density around V_S. The decrease of charge density may also cause the dissociation of H_2S to change into an exothermic process that can occur spontaneously. In addition, we found that after H_2S is completely disintegrated, the S atom fills the previous V_S, thus forming the perfect surface. According to this characteristic, we later put forward an evolution mechanism of sulfur vacancies on the FeS(001) surface.

2.4. Diffusion of H Atoms. H atoms generated by H_2S dissociation adsorb on the FeS(001) surface. By studying the diffusion mechanism of H atoms from the surface into the matrix by the DFT method, we can not only explore the hydrogen resistance performance of FeS but also further examine the influence mechanism of vacancy defects on H diffusion from the microscopic perspective.

Tables S2 and S3 list the E_{ads} and E_{dis} of H atoms and all possible diffusion paths of individual H atoms on the perfect FeS(001) surface. Table 3 shows the E_{ads} and E_{dis} of H atoms on vacancy-defective FeS(001) surfaces and the matrix. Except for the S-V site, the E_{ads} and E_{dis} of H atoms on the perfect and

Table 3. Adsorption Energy of the H Atom at Different Adsorption and Dissolution Sites on the Vacancy-Defective FeS(001) Surfaces

surfaces	adsorption site	E_{ads} (eV)
vacancy-defective-Fe FeS(001)	S-T	0.69
	Fe-B	0.71
	Fe-L	0.68
	S-L	0.59
vacancy-defective-S FeS(001)	S-T	0.94
	S-V	−0.84
	S-L	0.73

https://doi.org/10.1021/acsomega.1c02639
ACS Omega 2021, 6, 19212−19221

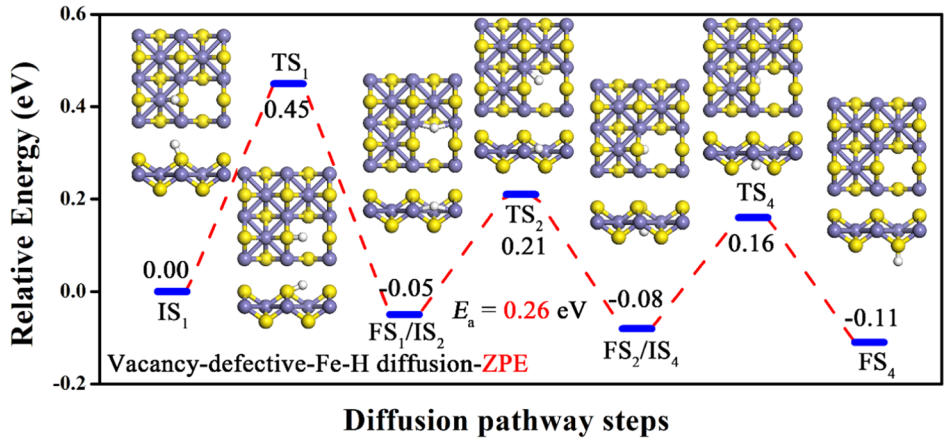

Figure 5. MEPs of the H diffusion process on the vacancy-defective-Fe FeS(001) surface.

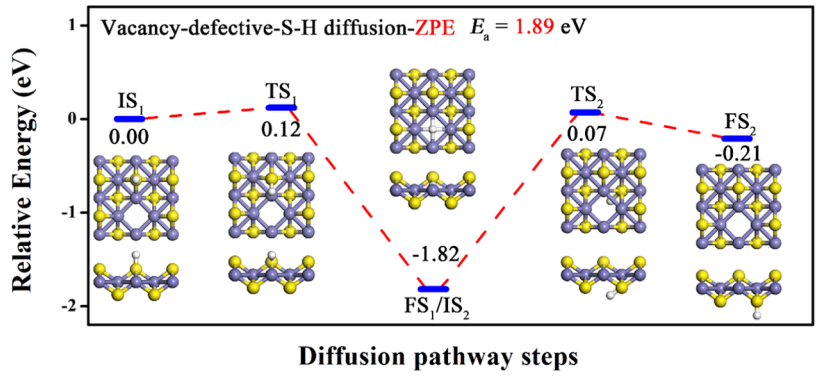

Figure 6. MEPs of the H diffusion process on the vacancy-defective-S FeS(001) surface.

vacancy-defective surfaces are both positive, which indicates that the adsorption/dissolution process of H atoms is not stable. At the S-V site, the adsorption energy of the H atom reaches −0.84 eV, which indicates that V_S has a great adsorption capacity for H atoms. As mentioned above, this is also caused by the decrease of the charge density around V_S.

Subsequently, we calculate all possible diffusion paths for H atoms on vacancy-defective FeS(001) surfaces. Figures S2, 5, and 6 show the MEPs of individual H atoms diffusing from the surface to the matrix on vacancy-defective FeS(001) surfaces. The illustration shows top and front views of the corresponding adsorption/dissolution locations and the configuration of the transition state. Table 4 lists E_a and ΔE with and without ZPE correction for all possible diffusion paths of H atoms on the FeS(001) surface. The bold fonts in Table 4 are E_a and ΔE of the rate-limiting steps for the H diffusion process into the matrix.

Table 4. Reaction Heat (ΔE) and Dissolution Energy Barrier (E_{dif}) for All Possible H Diffusion Paths on Vacancy-Defective FeS(001) Surfaces

	perform ZPE		no ZPE	
diffusion pathway steps	$E_{dif\text{-}ZPE}$ (eV)	$\Delta E_{\text{-}ZPE}$ (eV)	E_{dif} (eV)	ΔE (eV)
Vacancy-Defective-Fe FeS(001)				
P_1: S-T → Fe-B	0.45	−0.05	0.51	0.02
P_2: S-T → Fe-L	0.49	−0.07	0.55	−0.01
P_3: Fe-B → Fe-L	**0.26**	**−0.03**	**0.27**	**−0.03**
P_4: Fe-L → S-L	0.24	−0.03	0.22	−0.09
Vacancy-Defective-S FeS(001)				
P_1: S-T → S-V	0.12	−1.82	0.14	−1.78
P_2: S-V → S-L	**1.89**	**1.61**	**1.96**	**1.57**

On the perfect FeS(001) surface, the MEPs of H diffusion are S-T to Fe-B to Fe-L to S-L. The diffusion energy barrier E_a of the rate-limiting step of H diffusing into the matrix is 1.12 eV, which is not very large, thus H atoms can diffuse from the perfect FeS(001) surface into the matrix under certain conditions. The diffusion process of H atoms on the vacancy-defective-Fe FeS(001) surface is shown in Figure 5. According to the diffusion barrier, the MEPs of H diffusion are S-T to Fe-B to Fe-L to S-L, which is the same as H diffusion on the perfect surface. However, the energy barrier E_a of the rate-limiting step of diffusion is only 0.26 eV, which is overwhelmingly lower than that of the perfect surface (1.12 eV). It can be clearly seen from Figure 5 that the existence of V_{Fe} provides an expedited path for H atoms in the diffusion process. Thus, the diffusion process of H atoms is smoother and the diffusion energy barrier is lower. This is consistent with the steps of H diffusion in the H_2S dissociation process on the vacancy-defective-Fe FeS(001) surface calculated above, which further proves the rationality of this theory.

The H diffusion process on the vacancy-defective-S FeS(001) surface is shown in Figure 6. The adsorption sites of H atoms on the vacancy-defective-S FeS(001) surface are S-T and S-V. After calculation, we found that the diffusion of H atoms from S-T to S-V only needs to overcome a very small energy barrier of 0.12 eV, and unlike the S-T site, the adsorption of H atoms at the S-V site is an exothermic process. Therefore, it can be inferred that H atoms are very easy to

https://doi.org/10.1021/acsomega.1c02639
ACS Omega 2021, 6, 19212−19221

aggregate near V_S on the vacancy-defective-S FeS(001) surface. The energy barrier of H atom diffusion from S-V into the matrix is 1.89 eV, which is higher than that of the rate-limiting step on the perfect FeS(001) surface (1.12 eV). Different from V_{Fe}, the existence of V_S does not provide a smoother path for H diffusion. V_S binds the H atom to the vacancy defect, thus making the diffusion behavior of H atoms into the matrix more difficult, which is also caused by the decrease of charge density around V_S.

In summary, compared with the perfect FeS(001) surface, V_{Fe} and V_S have different influence mechanisms on the H atom diffusion process. V_{Fe} provides a smoother path for H atoms and considerably reduces the energy barrier of H diffusion into the matrix. On the other hand, the presence of V_S binds H atoms to V_S and hinders the diffusion of H atoms from the surface to the matrix.

2.5. Energy Barrier Split. The influence of vacancy defects on the H_2S dissociation and H diffusion process is shown in Figure 7. Compared with the perfect surface, V_{Fe} can promote

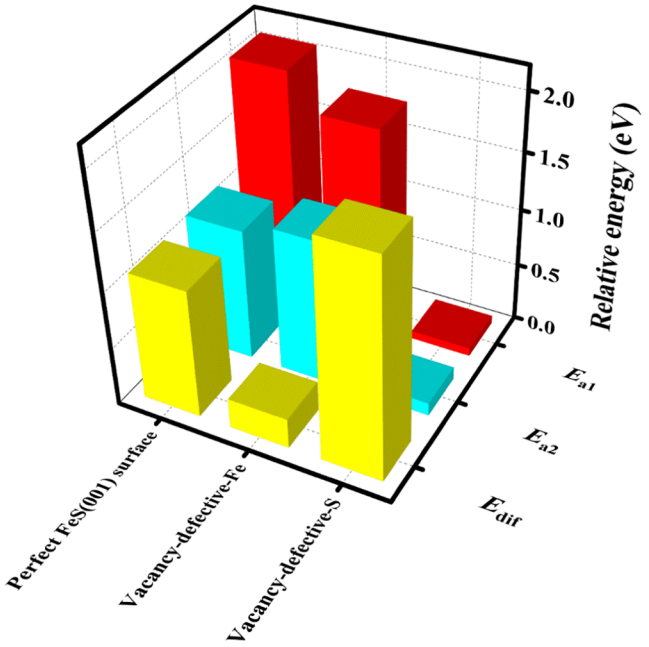

Figure 7. Diffusion barrier (E_{dif}) of H atoms and the dissociation barrier (E_a) of H_2S on perfect, vacancy-defective-Fe, and vacancy-defective-S FeS(001) surfaces.

the dissociation process of H_2S but hinder the dissociation of HS, while V_S has an extremely significant promoting effect on both H_2S and HS. In particular, V_S can also change the dissociation process of H_2S from an endothermic reaction, which is difficult to occur, to an exothermic reaction, which can proceed spontaneously. Furthermore, both V_{Fe} and V_S can promote the H diffusion process into the matrix, and the promotion effect of V_{Fe} is particularly significant.

According to the energy barrier splitting formula, each part contributes to the dissociation barrier E_a, as shown in Table 5. Compared with the perfect surface, the change of ΔE_{slab}, E_{TS1}^{HS}, E_{TS1}^{H}, $E_{IS1}^{H_2S}$, and $E_{int\text{-}H\cdots HS}$ on the vacancy-defective-Fe FeS(001) surface is small, but the change of $\Delta E_{def\text{-}H_2S}$ is obvious, which decreases by 0.46 eV. This is the main reason for the decrease of the dissociation barrier E_a of H_2S. On the vacancy-defective-S FeS(001) surface, the changes of E_{TS1}^{HS}, E_{TS1}^{H}, $E_{IS1}^{H_2S}$, and

Table 5. Contribution of Each Part to the Dissociation E_a of H_2S and HS

ΔE_{slab} (eV)	$\Delta E_{def\text{-}H_2S}$ (eV)	E_{TS1}^{HS} (eV)	E_{TS1}^{H} (eV)	$E_{IS1}^{H_2S}$ (eV)	$E_{int\text{-}H\cdots HS}$ (eV)
Perfect FeS(001)					
0.24	3.44	−0.76	0.66	−0.23	1.73
Vacancy-Defective-Fe FeS(001)					
0.22	2.98	−0.95	0.57	−0.19	1.45
Vacancy-Defective-S FeS(001)					
−0.02	0.02	−4.47	2.16	−1.21	−1.17
ΔE_{slab} (eV)	$\Delta E_{def\text{-}HS}$ (eV)	E_{TS2}^{S} (eV)	E_{TS2}^{H} (eV)	E_{IS2}^{HS} (eV)	$E_{int\text{-}H\cdots HS}$ (eV)
Perfect FeS(001)					
0.13	3.82	0.67	0.78	−1.27	5.52
Vacancy-Defective-Fe FeS(001)					
0.26	2.34	0.63	0.89	−1.43	4.30
Vacancy-Defective-S FeS(001)					
0.03	0.82	−3.97	−0.29	−4.83	1.31

$E_{int\text{-}H\cdots HS}$ are all significant, and their contribution together reduces the dissociation barrier E_a of H_2S. It is worth mentioning that compared with the perfect and vacancy-defective-Fe FeS(001) surfaces, the contribution of ΔE_{slab} and $\Delta E_{def\text{-}H_2S}$ to dissociation barrier E_a is very small, which indicates that the slab model and H_2S can move from the initial state to the transition state with little energy absorption. This also proves from the side that the configuration of H_2S after stable adsorption at the S vacancy defect mentioned above may be the precursor of H_2S dissociation. For the dissociation of HS, on the vacancy-defective-Fe surface, $\Delta E_{def\text{-}HS}$ decreases by 1.48 eV, which contributes the most to the dissociation barrier E_a. However, the interaction energy between H and S has a great positive contribution to the dissociation barrier E_a, which can almost cancel out the negative contribution of $\Delta E_{def\text{-}H_2S}$, so that the change of E_a is not very obvious. On the vacancy-defective-S surface, the changes of each part are manifested, which together lead to the decrease of the dissociation barrier E_a.

Based on the research results, we proposed an evolution mechanism of sulfur vacancies on the FeS(001) surface, as shown in Figure 8. In our opinion, V_S is very difficult to exist on the FeS(001) surface due to the following reasons: (a) The formation energy of V_S is very large and reaches 3.91 eV, which indicates that in the actual environment, it is difficult to form V_S on the FeS(001) surface under external conditions such as temperature and pressure. (b) Even if V_S was formed on the surface, H_2S in the environment would continue to spontaneously adsorb and dissociate at V_S, so as to fill V_S and form the perfect surface. Therefore, according to the calculation results, we propose that there is almost no V_S on the FeS(001) surface in a corrosive environment and the vast majority of V_S may exist within the matrix.

3. COMPUTATIONAL DETAILS

3.1. Models. The perfect and vacancy-defective FeS(001) surfaces are created through an utterly relaxed volume structure using Materials Studio (MS).[36] As shown in Figure S1a, the slab model of the FeS(001) surface adopts a 2 × 2 supercell structure and is equipped with nine atomic layers to adapt to the relaxation expansion of the first layer. An additional 15 Å vacuum layer is placed to ensure separation.[37,38] Zero-point energy (ZPE) correction is performed for the adsorption energy and dissociation energy

https://doi.org/10.1021/acsomega.1c02639
ACS Omega 2021, 6, 19212−19221

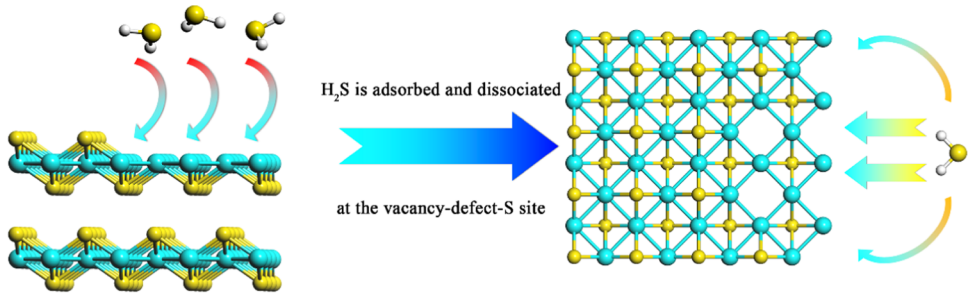

Figure 8. Evolution mechanism of S vacancies on the FeS(001) surface.

barriers.[39,40] In all calculations involving the interaction of H_2S and the dissociated atoms with the FeS(001) surface, the adsorbate and top three layers of atoms are totally allowed to relax, while the remaining atomic layers are fixed.

3.2. Methods. All of the calculations are executed using the Vienna Ab-initio Simulation Package (VASP).[41−45] The Perdew−Burke−Ernzerhof (PBE) generalized gradient approximation (GGA) exchange−correlation functional using the projector augmented wave method is applied.[46,47] We added the spin polarization parameters in the calculation process, which had little effect on the calculation of the perfect and vacancy-defective-Fe FeS(001) surfaces but had a great influence on the calculation of the vacancy-defective-S FeS(001) surface. Since the conventional DFT method cannot accurately describe the weak vdW force between atoms separated by vacuum, the DFT-D2 method is used to correct the weak vdW force between FeS layers in this study, which has been confirmed in other research studies.[27] When a cut-off energy of 400 eV is used, the total energy of FeS(001) converges. The *K*-points are set to be 11 × 11 × 11 for H_2S in vacuum and bulk FeS optimizations, while 5 × 5 × 1 is applied for FeS(001) surface calculations. The convergence standards of energy and force are 10^{-5} eV and 0.05 eV·Å^{-1}, respectively.

The formation energy of vacancy defects is defined by the following formula[48]

$$E_f = E_{V^{Fe}/V^S-FeS} - E_{FeS} + \mu i$$

Here, E_{V^{Fe}/V^S-FeS} and E_{FeS} denote the total energy of the FeS(001) model containing V_{Fe}/V_S and the perfect surface, respectively. The μi represents the atomic chemical potential introduced by the formation of V_{Fe}/V_S.

The transition state of the dissociation process of H_2S/HS and the H diffusion process is probed by a climbing image nudged elastic band (CI-NEB) method,[49] and the frequency of the transition state is checked to make sure there is only one virtual frequency. The formulas for adsorption/dissolution energy ($E_{ads/dis}$), ZPE correction, differential charge density (DCD), activation energy barrier (E_a), reaction heat (ΔE), and energy barrier splitting are all described in our published papers.[50]

4. CONCLUSIONS

Vacancy defects are inherent point defects of materials. Two kinds of vacancy defects on the FeS(001) surface can affect the adsorption/dissociation of H_2S and the H diffusion process. In our work, the impact of V_{Fe} and V_S on the adsorption/dissociation and diffusion of H_2S was calculated using the DFT-D2 method. In our calculation, V_{Fe} did not change the stable adsorption site and adsorption configuration of H_2S but promoted the dissociation process of H_2S. Compared with the perfect surface (2.08 eV), the dissociation energy barrier of H_2S was reduced to 1.56 eV. Meanwhile, V_{Fe} also slightly hindered the dissociation process of HS. V_S significantly promotes the adsorption and dissociation process of H_2S, which not only reduces the dissociation energy barriers of H_2S and HS to 0.07 and 0.11 eV, respectively, but also changes the dissociation process of H_2S from an endothermic process to a spontaneous exothermic one. In addition, V_{Fe} and V_S have different influence mechanisms on the H atom diffusion process. V_{Fe} provides a barrier-free diffusion channel for the diffusion process of H atoms, so the H diffusion process is more accessible. But the presence of V_S binds H atoms to V_S and hinders the diffusion of H atoms from the surface to the matrix. Compared with the perfect FeS(001) surface, the energy barriers of the rate-limiting step of H diffusion from the surface into the matrix on the vacancy-defective-Fe and vacancy-defective-S FeS(001) surfaces are 0.26 and 1.89 eV, respectively. In the end, according to the calculation results, we propose that there is almost no S vacancy defect existing on the FeS(001) surface in a corrosive environment. Our research provides a theoretical basis for understanding the influence of vacancy defects on the adsorption, dissociation, and diffusion processes of H_2S in FeS. Meanwhile, it can also provide a theoretical basis for the formation, transformation, and further corrosion of iron sulfide compounds. This may encourage scholars to conduct further experimental research and verification.

■ ASSOCIATED CONTENT

Supporting Information

The Supporting Information is available free of charge at https://pubs.acs.org/doi/10.1021/acsomega.1c02639.

Model of layered FeS and different adsorption sites of vacancy-defective-Fe and vacancy-defective-S FeS(001) surfaces; adsorption energy, adsorption sites, and structural parameters of H_2S, HS, S, and H stably adsorbed on different FeS(001) surfaces; adsorption energy of the H atom at different adsorption and dissolution sites on the perfect FeS(001) surface; dissolution energy barrier (E_{dif}) and reaction heat (ΔE) for all possible diffusion paths of the H atom; and MEPs of the H atom diffusing on the perfect FeS(001) surface (PDF)

■ AUTHOR INFORMATION

Corresponding Author

Shuqi Zheng − *School of New Energy and Materials, China University of Petroleum (Beijing), Beijing 102249, P. R. China;* orcid.org/0000-0003-1549-8000; Phone: +86

https://doi.org/10.1021/acsomega.1c02639
ACS Omega 2021, 6, 19212−19221

010 8973 3200; Email: zhengsq09@163.com; Fax: +86 010 8973 3200

Authors

Jingxuan Liang − *School of New Energy and Materials, China University of Petroleum (Beijing), Beijing 102249, P. R. China*

Xiangli Wen − *School of New Energy and Materials, China University of Petroleum (Beijing), Beijing 102249, P. R. China; State Key Laboratory of Tribology, Department of Mechanical Engineering, Tsinghua University, Beijing 100084, P. R. China*

Shikai Wei − *School of New Energy and Materials, China University of Petroleum (Beijing), Beijing 102249, P. R. China*

Complete contact information is available at: https://pubs.acs.org/10.1021/acsomega.1c02639

Notes

The authors declare no competing financial interest.

■ ACKNOWLEDGMENTS

This work was financially supported by the National Natural Science Foundation of China (No. 51671215) and the Seed Fund for International Cooperation of China University of Petroleum, Beijing. The calculations were carried out at the National Supercomputing Center in Shenzhen (Shenzhen Cloud Computing Center).

■ REFERENCES

(1) Wang, Z.; Feng, Z.; Zhang. Effect of high temperature on the corrosion behavior and passive film composition of 316 L stainless steel in high H_2S-containing environments. *Corros. Sci.* **2020**, *174*, No. 108844.

(2) Xie, C.; Wang, B.; Li, S.; Wen, X.; Wei, S.; Zhang, S.; Feng, M.; Chen, L.; Zheng, S. The dependence of anti-corrosion behaviors of iron sulfide films on different reactants. *Int. J. Hydrogen Energy* **2020**, *45*, 17548−17556.

(3) Wei, S.; Zheng, S.; Xie, C.; Liang, J. Ab initio molecular dynamics study of wet H_2S adsorption and dissociation on Fe(100) surface. *J. Mol. Liq.* **2020**, *319*, No. 114135.

(4) Abd El Haleem, S. M.; Abd El Aal, E. E. Electrochemical behaviour of iron in alkaline sulphide solutions. *Corros. Eng., Sci. Technol.* **2008**, *43*, 173−178.

(5) Pound, B. G.; Wright, G. A.; Sharp, R. M. The anodic behavior of iron in hydrogen sulfide solutions. *Corrosion* **1989**, *45*, 386−392.

(6) Rickard, D.; Luther, G. W. Chemistry of iron sulfides. *Chem. Rev.* **2007**, *107*, 514−562.

(7) Benning, L. G.; Wilkin, R. T.; Barnes, H. L. Reaction pathways in the Fe−S system below 100 °C. *Chem. Geol.* **2000**, *167*, 25−51.

(8) Livens, F. R.; Jones, M. J.; Hynes, A. J.; Charnock, J. M.; Mosselmans, J. F.; Hennig, C.; Steele, H.; Collison, D.; Vaughan, D. J.; Pattrick, R. A.; Reed, W. A.; Moyes, L. N. X-ray absorption spectroscopy studies of reactions of technetium, uranium and neptunium with mackinawite. *J. Environ. Radioact.* **2004**, *74*, 211−219.

(9) Wen, X.; Liang, Y.; Bai, P.; Luo, B.; Fang, T.; Yue, L.; An, T.; Song, W.; Zheng, S. First-principles calculations of the structural, elastic and thermodynamic properties of mackinawite (FeS) and pyrite (FeS_2). *Phys. B* **2017**, *525*, 119−126.

(10) Bai, P.; Zheng, S.; Chen, C.; Zhao, H. Investigation of the Iron−Sulfide Phase Transformation in Nanoscale. *Cryst. Growth Des.* **2014**, *14*, 4295−4302.

(11) Bai, P.; Zheng, S.; Chen, C. Electrochemical characteristics of the early corrosion stages of API X52 steel exposed to H_2S environments. *Mater. Chem. Phys.* **2015**, *149−150*, 295−301.

(12) Bai, P.; Liang, Y.; Zheng, S.; Chen, C. Effect of Amorphous FeS Semiconductor on the Corrosion Behavior of Pipe Steel in H_2S-Containing Environments. *Ind. Eng. Chem. Res.* **2016**, *55*, 10932−10940.

(13) Wen, X.; Bai, P.; Luo, B.; Zheng, S.; Chen, C. Review of recent progress in the study of corrosion products of steels in a hydrogen sulphide environment. *Corros. Sci.* **2018**, *139*, 124−140.

(14) Taylor, P.; Rummery, T. E.; Owen, D. G. Reactions of iron monosulfide solids with aqueous hydrogen sulfide up to 160 °C. *J. Inorg. Nucl. Chem.* **1979**, *41*, 1683−1687.

(15) Li, Y.; Van Santen, R. A.; Weber, T. High-temperature FeS−FeS_2 solid-state transitions: Reactions of solid mackinawite with gaseous H_2S. *J. Solid State Chem.* **2008**, *181*, 3151−3162.

(16) Folena, M. C.; da Cunha Ponciano, J. A. Assessment of hydrogen embrittlement severity of an API 5LX80 steel in H_2S environments by integrated methodologies. *Eng. Failure Anal.* **2020**, *111*, No. 104380.

(17) Bai, P-p.; Zhou, J.; Luo, B-w.; Zheng, S-q.; Wang, P-y.; Tian, Y. Hydrogen embrittlement of X80 pipeline steel in H_2S environment: Effect of hydrogen charging time, hydrogen-trapped state and hydrogen charging−releasing−recharging cycles. *Int. J. Miner., Metall. Mater.* **2020**, *27*, 63−73.

(18) Lennie, A. R.; Redfern, S.; Schofield, P.; Vaughan, D. J. Synthesis and Rietveld crystal structure refinement of mackinawite, tetragonal FeS. *Mineral. Mag.* **1995**, *59*, 677−683.

(19) Jeong, H. Y.; Lee, J. H.; Hayes, K. F. Characterization of synthetic nanocrystalline mackinawite: crystal structure, particle size, and specific surface area. *Geochim. Cosmochim. Acta* **2008**, *72*, 493−505.

(20) Dzade, N. Y.; Roldan, A.; de Leeuw, N. H. The surface chemistry of NO_x on mackinawite (FeS) surfaces: a DFT-D2 study. *Phys. Chem. Chem. Phys.* **2014**, *16*, 15444−15456.

(21) Dzade, N. Y.; Roldan, A.; de Leeuw, N. H. Activation and dissociation of CO_2 on the (001), (011), and (111) surfaces of mackinawite (FeS): A dispersion-corrected DFT study. *J. Chem. Phys.* **2015**, *143*, No. 094703.

(22) Dzade, N. Y.; Roldan, A.; de Leeuw, N. H. DFT-D2 simulations of water adsorption and dissociation on the low-index surfaces of mackinawite (FeS). *J. Chem. Phys.* **2016**, *144*, No. 174704.

(23) Dzade, N. Y.; de Leeuw, N. H. Adsorption and desulfurization mechanism of thiophene on layered fes (001), (011), and (111) surfaces: A dispersion-corrected density functional theory study. *J. Phys. Chem. C* **2018**, *122*, 359−370.

(24) Dzade, N. Y.; Roldan, A.; de Leeuw, N. H. Surface and shape modification of mackinawite (FeS) nanocrystals by cysteine adsorption: a first-principles DFT-D2 study. *Phys. Chem. Chem. Phys.* **2016**, *18*, 32007−32020.

(25) Dzade, N. Y.; Roldan, A.; de Leeuw, N. H. DFT-D2 study of the adsorption and dissociation of water on clean and oxygen-covered {001} and {011} surfaces of mackinawite (FeS). *J. Phys. Chem. C* **2016**, *120*, 21441−21450.

(26) Krishnamoorthy, A.; Dinh, M. A.; Yildiz, B. Hydrogen weakens interlayer bonding in layered transition metal sulfide $Fe_{1+x}S$. *J. Mater. Chem. A* **2017**, *5*, 5030−5035.

(27) Wen, X.; Bai, P.; Zheng, S.; Tian, Y. Adsorption and dissociation mechanism of hydrogen sulfide on layered FeS surfaces: A dispersion-corrected DFT study. *Appl. Surf. Sci.* **2021**, *537*, No. 147905.

(28) Vekilova, O. Y.; Bazhanov, D. I.; Simak, S. I.; Abrikosov, I. A. First-principles study of vacancy-hydrogen interaction in Pd. *Phys. Rev. B* **2009**, *80*, No. 024101.

(29) Liu, Y.-L.; Zhang, Y.; Zhou, H.-B.; Lu, G.-H.; Liu, F.; Luo, G.-N. Vacancy trapping mechanism for hydrogen bubble formation in metal. *Phys. Rev. B* **2009**, *79*, No. 172103.

(30) Nguyen, H. T.; Minh, N. Effects of Sulfur-Deficient Defect and Water on Rearrangements of Formamide on Pyrite (100) Surface. *J. Phys. Chem. A* **2014**, *118*, 4079−4086.

(31) Galvez-Martinez, S.; Elizabeth, E.-R.; Maria-Paz, Z.; Eva, M.-M. Defects on a Pyrite (100) Surface Produce Chemical Evolution of

Glycine under Inert Conditions: Experimental and Theoretical Approaches. *Phys. Chem. Chem. Phys.* **2019**, *21*, 24535−24542.
(32) Sahraei, A. A.; Faïçal, L. How Do Surface Defects Change Local Wettability of the Hydrophilic Zns Surface? Insights into Sphalerite Flotation from Density Functional Theory Calculations. *J. Phys. Chem. C* **2021**, *125*, 998−1009.
(33) Sahraei, A. A.; Faïçal, L. Chemical Transformation and Dissociation of Amino Acids on Metal Sulfide Surface: Insights from Dft into the Effect of Surface Vacancies on Alanine-Sphalerite System. *Appl. Surf. Sci.* **2021**, *540*, No. 148304.
(34) Ward, J. C. The structure and properties of some iron sulphides *Rev. Pure Appl. Chem.* 1970, 175−206.
(35) Taylor, L. A.; Finger, L. W. *Structural Refinement and Composition of Mackinawite*; Carnegie Instution of Washington, Geophysical Laboratory Annual Report, 1970; Vol. *69*, pp 318−322.
(36) Pilot, P. version 7.0; Accelrys Inc.: San Diego, CA, 2013.
(37) Han, Z.; Yu, H.; Li, C.; Zhou, S. Mulch-assisted ambient-air synthesis of oxygen-rich activated carbon for hydrogen storage: A combined experimental and theoretical case study. *Appl. Surf. Sci.* **2021**, *544*, No. 148963.
(38) Han, Z.; Wu, Y.; Yu, H.; Zhou, S. Location-dependent effect of nickel on hydrogen dissociation and diffusion on Mg (0001) surface: Insights into hydrogen storage material design. *J. Magnesium Alloys* **2021**, DOI: 10.1016/j.jma.2021.03.002.
(39) Cahyanto, W. T.; Zulaehah, S.; Widanarto, W.; Abdullatif, F.; Effendi, M.; Kasai, H. Theoretical Study of an almost Barrier-Free Water Dissociation on a Platinum (111) Surface Alloyed with Ruthenium and Molybdenum. *ACS Omega* **2021**, *6*, 10770−10775.
(40) Vakili, M.; Gholizadeh, R.; Ghadi, A.; Salmasi, E.; Sinnokrot, M. Computational investigation of N_2O adsorption and dissociation on the silicon-embedded graphene catalyst: A density functional theory perspective. *J. Mol. Graphics Modell.* **2020**, *101*, No. 107752.
(41) Kresse, G.; Hafner, J. Ab initio molecular dynamics for open-shell transition metals. *Phys. Rev. B* **1993**, *48*, 13115−13118.
(42) Kresse, G.; Hafner, J. Norm-conserving and ultrasoft pseudopotentials for first-row and transition elements. *J. Phys.: Condens. Matter* **1994**, *6*, 8245−8257.
(43) Kresse, G.; Furthmüller, J. Efficiency of ab-initio total energy calculations for metals and semiconductors using a plane-wave basis set. *Comput. Mater. Sci.* **1996**, *6*, 15−50.
(44) Kresse, G.; Furthmüller, J. Efficient iterative schemes for ab initio total-energy calculations using a plane-wave basis set. *Phys. Rev. B* **1996**, *54*, 11169−11186.
(45) Wei, S.; Zheng, S.; Wen, X.; Xie, C.; Liang, J. A novel antiferromagnetic semiconductor hidden in pyrite. *Comput. Mater. Sci.* **2020**, *183*, No. 109852.
(46) Blöchl, P. E. Projector augmented-wave method. *Phys. Rev. B* **1994**, *50*, 17953−17979.
(47) Kresse, G.; Joubert, D. From ultrasoft pseudopotentials to the projector augmented-wave method. *Phys. Rev. B* **1999**, *59*, 1758−1775.
(48) Chen, D.; Zhang, X.; Tang, J.; Cui, H.; Pi, S.; Cui, Z. Adsorption of SF_6 Decomposed Products over ZnO(1010): Effects of O and Zn Vacancies. *ACS Omega* **2018**, *3*, 18739−18752.
(49) Peng, M.; Wang, Y.; Han, Y.; Ye, C.; Zou, J.-J.; Li, W.; Zhang, J. Cu-Si bond and Cl defect synergistical catalysis for $SiCl_4$ dissociation on $CuCl_2$(100): A DFT study. *Appl. Surf. Sci.* **2021**, *543*, No. 148777.
(50) Wen, X.; Bai, P.; Han, Z.; Zheng, S.; Luo, B.; Fang, T.; Song, W. Effect of vacancy on adsorption/dissociation and diffusion of H_2S on Fe(100) surfaces: A density functional theory study. *Appl. Surf. Sci.* **2019**, *465*, 833−845.

https://doi.org/10.1021/acsomega.1c02639
ACS Omega 2021, 6, 19212−19221